[CANCER RESEARCH 64, 2502–2508, April 1, 2004]

Dependence of Paclitaxel Sensitivity on a Functional Spindle Assembly Checkpoint

Tamotsu Sudo,[1] Masayuki Nitta,[3] Hideyuki Saya,[3] and Naoto T. Ueno[1,2]

[1]Breast Cancer Research Program Core Laboratory, Department of Blood and Marrow Transplantation and [2]Department of Molecular and Cellular Oncology, The University of Texas M. D. Anderson Cancer Center, Houston, Texas, and [3]Department of Tumor Genetics and Biology, Graduate School of Medical Sciences, Kumamoto University, Kumamoto, Japan

ABSTRACT

Paclitaxel stabilizes microtubules, causing mitotic arrest and activating the spindle assembly checkpoint. We determined whether suppression of the checkpoint genes *Mad2* and *BubR1* affects paclitaxel resistance and whether overexpression of Mad2 protein in checkpoint-defective cells enhances paclitaxel sensitivity. Suppression of *Mad2* and *BubR1* in paclitaxel-treated cancer cells abolished checkpoint function, resulting in paclitaxel resistance that correlated with suppression of cyclin-dependent kinase-1 activity. In contrast, overexpression of Mad2 in cells with a checkpoint defect attributable to low Mad2 expression restored checkpoint function, resulting in enhanced paclitaxel sensitivity that correlated with enhanced cyclin-dependent kinase-1 activity. However, overexpression of Mad2 failed to enhance paclitaxel sensitivity via checkpoint activation in Mad2-independent checkpoint-defective and -intact cells. Thus, checkpoint function is required for paclitaxel sensitivity. These findings show that any molecules that could interfere with the spindle assembly checkpoint could generate paclitaxel resistance in any patient.

INTRODUCTION

Paclitaxel (Taxol) is widely used in the treatment of breast, ovarian, and other solid tumors. Randomized clinical trials have shown a survival advantage among patients with primary breast cancer who received paclitaxel in addition to anthracycline-containing adjuvant chemotherapy (1). Furthermore, paclitaxel is effective for both metastatic breast cancer (2–4) and advanced ovarian cancer (5, 6). However, some patients are resistant to paclitaxel therapy, and the characteristics of patients who will benefit from the drug have not been well defined. Identification of molecular characteristics predictive of paclitaxel sensitivity or resistance could aid in selecting patients to receive this therapy.

Previous reports have demonstrated that paclitaxel resistance is attributable to a variety of mechanisms: up-regulation of antiapoptotic Bcl-2 family members, such as Bcl-2 and Bcl-X_L (7); up-regulation of membrane transporters (*e.g.*, mdr-1), resulting in an increased drug efflux (8); mutations in β-tubulin, resulting in abolishment of paclitaxel binding (9); and up-regulation of ErbB2 (HER-2) through inhibition of cyclin-dependent kinase-1 (Cdk1), resulting in delayed mitosis (10).

Two molecules that might be related to paclitaxel resistance are the spindle assembly checkpoint and Cdk1. When paclitaxel stabilizes microtubules and interferes with the dynamic changes that occur during formation of the mitotic spindle, the spindle assembly checkpoint is activated to make cells arrest at mitosis (11). This checkpoint monitors both the attachment of chromosomes to the mitotic spindle and the tension across the sister chromatid generated by microtubules to prevent premature chromosomal segregation. The molecular components of the spindle assembly checkpoint were initially identified in *Saccharomyces cerevisiae*. Mammalian homologues of the checkpoint proteins include Mad1, Mad2, BubR1, Bub3, and Mps1 (12–15). The target of this checkpoint is the anaphase-promoting complex (APC) and its coactivator Cdc20. Mad2 and BubR1 are located downstream and appear to be the major proteins of this machinery, interacting with Cdc20 directly and inhibiting APC activity cooperatively (16–19). However, the relationship between the spindle assembly checkpoint and paclitaxel sensitivity remains unclear.

Cdk1, combined with mitotic cyclins, is a universal master kinase required for regulation of mitosis (20). Cdk1 activity is maximized in accordance with activation of the spindle assembly checkpoint. Previous reports using either a Cdk inhibitor or dominant-negative Cdk1 have shown that Cdk1 is critical for paclitaxel-induced cell death (21, 22). However, whether activation of Cdk1 is the cause or the consequence of activated checkpoint activation remains unclear.

In this study, we sought to determine whether the spindle assembly checkpoint is required for paclitaxel sensitivity.

MATERIALS AND METHODS

Cell Lines and Cell Culture. All human cell lines used in this study—HEK 293 cells, for development of the recombinant plasmid; MCF-7 breast cancer and MCF-10A normal mammary cells, which are known to have a functional spindle assembly checkpoint; and T47D breast cancer and Ovca432 ovarian cancer cells, which have a defective checkpoint because of low Mad2 expression—were obtained from the American Type Culture Collection (Rockville, MD). HEK 293, MCF-7, and T47D cells were grown in DMEM:Ham's F-12 medium. Ovca432 cells were maintained in RPMI 1640. Both DMEM:Ham's F-12 medium and RPMI 1640 were supplemented with 2 mM L-glutamine, 10% fetal bovine serum (100 IU/ml), and penicillin-streptomycin (100 mg/ml). MCF-10A cells were maintained in DMEM:Ham's F-12 medium supplemented with 5% horse serum, 0.02 μg/ml epidermal growth factor, 0.5 μg/ml hydrocortisone, 10 μg/ml insulin, 0.1 μg/ml cholera toxin, 100 IU/ml penicillin, and 100 mg/ml streptomycin.

Small-Interfering RNA (siRNA) Transfection. Twenty-one nucleotide siRNA duplexes were synthesized by Dharmacon Research, Inc. (Lafayette, CO), to target the *Mad2* sequence 5′-AAACCTTTACTCGAGTGCAGA-3′ and the *BubR1* sequence 5′-AACAATACTCTTCAGCAGCAG-3′. Transfections of MCF-7 cells were performed in accordance with the protocol provided by Dharmacon Research using oligofectamine transfection reagent (Invitrogen, Carlsbad, CA). For the control experiments, cells were transfected with a siRNA-scrambled duplex (Dharmacon Research). The final concentration for the siRNAs was 200 nM.

Production of Replication-Defective Recombinant Adenovirus. The adenovirus was produced in accordance with the protocol described by Dr. Vogelstein's group (23) and Stratagene (La Jolla, CA). Briefly, the gene of cDNA Mad2 was first cloned into a shuttle vector, pAdTrack-cytomegalovirus. The resultant plasmid was linearized by digestion with restriction endonuclease Pme I and subsequently cotransformed into *Escherichia coli* BJ5183 cells using an adenoviral backbone plasmid, pAdEasy-1 (Stratagene). Recombinants were selected for kanamycin resistance, and recombination was confirmed by restriction endonuclease analyses. Finally, HEK 293 cells were transfected with the linearized recombinant plasmid. For our study, an infection efficiency of 80–90%, with no cytopathic effect, was obtained in each cell.

Western Blot Analysis. At 24, 48, and 72 h after transfection, cells were harvested and subjected to protein immunoblot analysis. Cells were washed once in ice-cold PBS and lysed with lysis buffer [1% NP40, 150 mM NaCl, and 50 mM Tris-HCl (pH 7.5)] containing protease inhibitors (1 mM phenylmethane

Received 7/7/03; revised 12/23/03; accepted 1/20/04.

Grant support: T. Sudo is supported by a research fellowship from the Uehara Memorial Foundation.

The costs of publication of this article were defrayed in part by the payment of page charges. This article must therefore be hereby marked *advertisement* in accordance with 18 U.S.C. Section 1734 solely to indicate this fact.

Requests for reprints: Naoto T. Ueno, Department of Blood and Marrow Transplantation, The University of Texas M. D. Anderson Cancer Center, Houston, TX 77030. Phone: (713) 792-8754; Fax (713) 794-4747; E-mail: nueno@mdanderson.org.

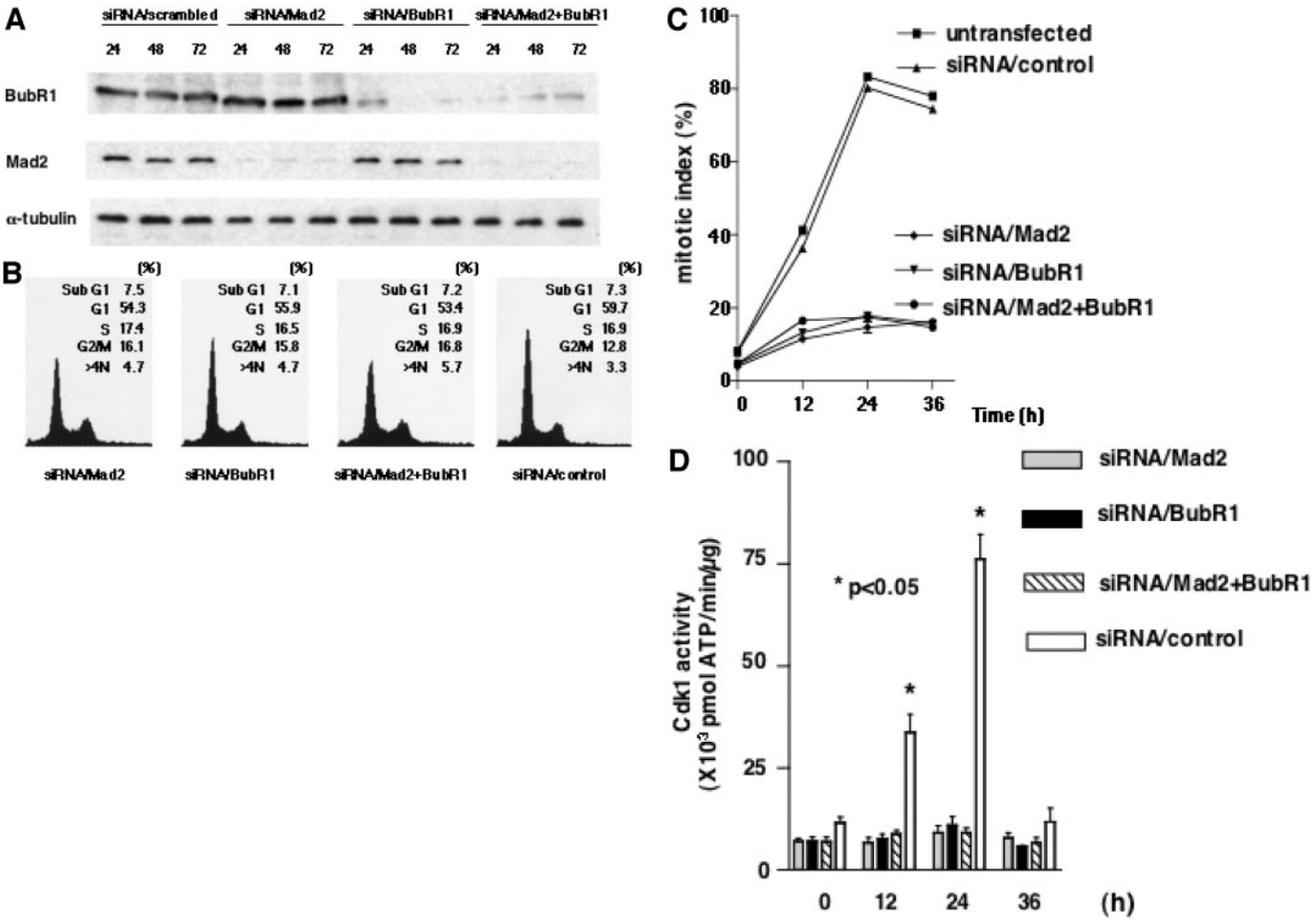

Fig. 1. Loss of spindle assembly checkpoint in cells with suppression of Mad2, BubR1, or both. *A*, reduction of BubR1 and Mad2 levels after transfection with small-interfering siRNA (siRNA). MCF-7 cells were transfected with siRNA/*Mad2* or siRNA/*BubR1*, resulting in a final concentration of 200 nM for the siRNAs. At the indicated times after transfection, cells were harvested and subjected to protein immunoblot analysis with each antibody and α-tubulin antibody to control for gel loading. *B*, no difference in cell cycle distribution by suppression of BubR1, MAD2, or both. Cell cycle distribution of cells with suppression of Mad2, BubR1, or both, as measured by DNA content by fluorescence-activated cell sorting as described in "Materials and Methods." MCF-7 cells were transfected and harvested 72 h after transfection. *Numbers* indicate percentages of cells in each phase. Nonstatistical significance was determined in each cell line by χ^2 test ($P = 0.0514$). *C*, reduction of mitotic indices of each cell by suppression of BubR1, MAD2, or both after treatment with paclitaxel. Twenty-four h after transfection, cells were treated with paclitaxel (100 nM) and harvested at the indicated times. *Bars*, SDs. *D*, suppression of cyclin-dependent kinase-1 (Cdk1) activity by suppression of BubR1, MAD2, or both after treatment with paclitaxel in each cell line. Twenty-four h after transfection, cells were treated with paclitaxel (100 nM) and harvested at the indicated times. Activity of Cdk1 in the lysates was determined as described in "Materials and Methods." *Bars*, SDs.

sulfonyl fluoride and 10 μg/ml aprotinin) and phosphatase inhibitors (20 mM β-glycerophosphate, 5 mM NaF, and 100 μM Na_3VO_4). After 30 min on ice, cells were subjected to centrifugation at 13,000 rpm for 15 min at 4°C. For Western blotting, equal amounts of proteins were dissolved using SDS-PAGE and transferred to nitrocellulose membranes. The membranes were incubated with polyclonal anti-Mad2 antibody (1:500; Covance, Princeton, NJ), monoclonal anti-BubR1 antibody (1:500; Chemicon, Temecula, CA), and monoclonal anti-α-tubulin (1:5000; Sigma-Aldrich Chemical Co., St. Louis, MO) for 1 h at room temperature (or overnight at 4°C), followed by incubation with horseradish peroxidase-conjugated antibodies. The results were visualized with the enhanced chemiluminescence detection system.

Drug Sensitivity Assays. Cells were detached by trypsinization, seeded at 2.0×10^3 cells/well in a 96-well microtiter plate, and treated with various concentrations of paclitaxel (1, 5, 10, 50, 100, and 1000 nM). Seventy-two h later, the effects on cell growth were examined by 3-(4,5-dimethylthiazol-2-yl)-2,5-diphenyltetrazolium bromide assay; 20 μl of 3-(4,5-dimethylthiazol-2-yl)-2,5-diphenyltetrazolium bromide solution (5 mg/ml in PBS; Sigma-Aldrich) were added to each well, and the cells were incubated for 4 h at 37°C. The 3-(4,5-dimethylthiazol-2-yl)-2,5-diphenyltetrazolium bromide-formazan formed by metabolically viable cells was dissolved in 100 μl of cell lysis buffer, and fluorescence was monitored using a microplate at a wavelength of 570 nm. The percentage of cell growth was calculated by defining the absorption of cells not treated with paclitaxel (control) as 100%.

Calculation of Mitotic Indices. Cells with mitotic condensed chromatin were visualized by staining with 10 μM Hoechst 33342 dye (Aventis Pharmaceuticals Inc., Bridgewater, NJ) in conjunction with 10 μg/ml propidium iodide; the propidium iodide was incorporated into dead cells only. Therefore, dead cells were stained with both propidium iodide and Hoechst 33342 dye, whereas mitotic cells showed the condensed chromatins with Hoechst 33342 dye only. The cells were harvested at 12, 24, and 36 h after transfection and the mitotic indices calculated. Results are presented after at least three independent experiments performed in triplicate.

Cell Death Analysis. Cell death was evaluated using the trypan blue dye exclusion assay. Briefly, cells were harvested using trypsin and stained with 0.4% trypan blue dye (Sigma-Aldrich). Trypan blue-positive and -negative cells were counted using a hemacytometer (Hausser Scientific, Horsham, PA) under a phase-contrast microscope (Fisher Scientific, Pittsburgh, PA). The results of each assay were expressed in terms of the percentage of dead cells relative to the total number of cells. Individual experiments were performed in triplicate. The results were reported as the mean values ±SDs. Presented results reflect at least three independent experiments performed in triplicate.

Cdk1 Kinase Assay. The Cdk1 protein kinase assay was performed using the SignaTECT cdc2 protein assay system (Promega, Madison, WI). Briefly, the harvested cells were lysed with the extraction buffer [50 mM Tris (pH 7.4), 150 mM NaCl, 0.1% Triton X-100, and 1 mM EDTA] containing protease inhibitors (100 μg/ml aprotinin and 0.5 mM phenylmethane sulfonyl fluoride)

and phosphatase inhibitors (50 mM NaF). These lysates were conjugated with a substrate consisting of cdc2-specific biotinylated peptide derived from histone H1 and [γ-^{32}P]ATP, and incubated at 30°C for 10 min. These radiolabeled, phosphorylated substrates were recovered with streptavidin matrix biotin capture membrane (SAM; Promega). After several washings, each captured membrane was placed into a separate vial and analyzed using a liquid scintillation counter (Beckman Coulter, Palo Alto, CA). Presented results reflect at least three independent experiments performed in triplicate.

RESULTS

Inactivation of Spindle Assembly Checkpoint and Correlation with Suppression of Cdk1 Activity. Transfection of MCF-7 cells, which have a functional checkpoint, with the 21-nucleotide siRNA duplex homologous to a portion of the *Mad2* and *BubR1* sequences resulted in dramatic reduction of Mad2 and BubR1 protein levels; these levels remained low at 24, 48, and 72 h after transfection in each cell line. Cotransfection of MCF-7 cells with siRNA/*Mad2* and siRNA/*BubR1* also reduced both expressions, yielding results similar to those obtained with single transfection (Fig. 1*A*). The scrambled siRNA duplex (siRNA/control) did not affect the expression level of Mad2 or BubR1, verifying the specificity of the siRNA approach.

Using flow cytometry, we attempted to determine whether transient suppression of mitotic checkpoint genes by siRNA affects the cell cycle distribution. Seventy-two h after transfection, there were no statistically significant differences in cell cycle distributions in neither the Mad2- nor the BubR1-suppressed cells ($P = 0.514$; Fig. 1*B*). To test the effects of suppression of Mad2, BubR1, or both on the spindle assembly checkpoint activated by paclitaxel, we determined the mitotic indices and measured the Cdk1 activity, both of which reflect the status of this checkpoint. Twenty-four h after paclitaxel treatment, at least 80% of the control cells were arrested at mitosis and showed a dramatic increase in Cdk1 activity, thus verifying activation of the spindle assembly checkpoints (Fig. 1, *C* and *D*). In contrast, the accumulation of mitotic indices and activation of Cdk1 were suppressed in Mad2- and BubR1-suppressed cells at 12 and 24 h ($P < 0.05$; Fig. 1, *C* and *D*). However, at 36 h, there is a reduction of Cdk1 activity in control cells attributable to induction of cell death by paclitaxel. Interestingly, concurrent suppression of Mad2 and BubR1 showed loss of accumulation of mitotic indices and activation of Cdk1, results similar to those obtained with suppression of either Mad2 or BubR1 alone (Fig. 1, *C* and *D*). These results indicate that Mad2 or BubR1 alone was sufficient to abolish the function of the spindle assembly checkpoint. This abolishment was reflected by suppression of Cdk1 activity.

Loss of Spindle Assembly Checkpoint and Paclitaxel Resistance. To determine the effect of loss of the spindle assembly checkpoint attributable to suppression of Mad2, BubR1, or both on paclitaxel sensitivity, we compared the cell viability of paclitaxel using the 3-(4,5-dimethylthiazol-2-yl)-2,5-diphenyltetrazolium bromide assay. As shown in Fig. 2*A*, MCF-7 cells in which Mad2, BubR1, or both were suppressed were more resistant to paclitaxel than were control cells. Next, to determine whether these resistances were attributable to the reduction of cell death induced by paclitaxel, we assessed the population of cell death using trypan blue exclusion. Forty-eight h after treatment with paclitaxel, levels of cell death were high in control cells but reduced in the cells in which Mad2, BubR1, or both were suppressed ($P < 0.05$; Fig. 2*B*). These data demonstrate that loss of the spindle assembly checkpoint increases paclitaxel resistance.

Effect of Mad2 Overexpression on Cdk1 Activity and Paclitaxel Sensitivity in Mad2-Dependent, Checkpoint-Defective Cells. Although *Mad2* mutations have not been detected in cancer cell lines with checkpoint defects (24), the expression level of Mad2 protein

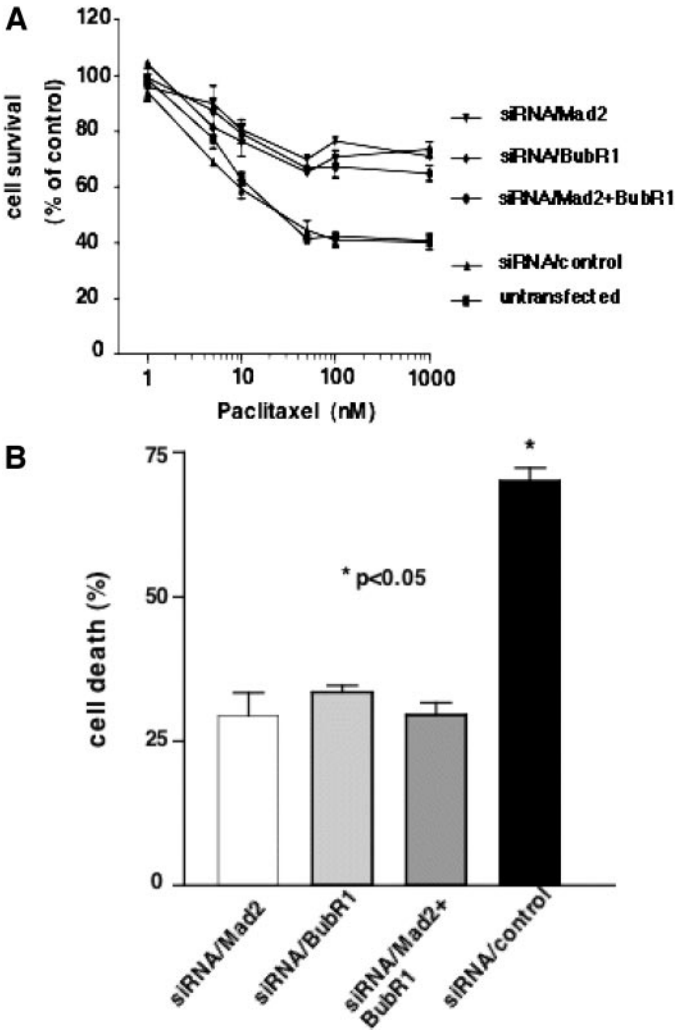

Fig. 2. Induction of paclitaxel resistance via loss of spindle assembly checkpoint. *A*, increased paclitaxel resistance by suppression of BubR1, MAD2, or both. MCF-7 cells transfected with small-interfering RNA (siRNA)/*Mad2*, *BubR1*, or both were examined using 3-(4,5-dimethylthiazol-2-yl)-2,5-diphenyltetrazolium bromide assay to determine the effects of paclitaxel on cell growth. Twelve h after transfection, the cells were detached by trypsinization. Twelve h after seeding, cells were treated with paclitaxel at various concentrations. *Bars*, SDs. *B*, decreased paclitaxel-induced cell death by suppression of BubR1, MAD2, or both. MCF-7 cells transfected with siRNA/*Mad2*, *BubR1*, or both were examined for cell death induced by paclitaxel. Twenty-four h after transfection, cells were treated with paclitaxel (100 nM) for 48 h. Cell viability was assessed using trypan blue exclusion assay. *Bars*, SDs.

appears to correlate with the competence of the spindle assembly checkpoint (25, 26). Therefore, we sought to determine whether overexpression of Mad2 restores spindle assembly checkpoint activation in cells in which low Mad2 expression renders the spindle assembly checkpoint nonfunctional. To express Mad2 effectively, we generated the recombinant adenovirus that expresses Mad2 (Ad-*EGFP/Mad2*). This adenovirus contains two independent cytomegalovirus-driven transcription units (one for *GFP* and one for *Mad2*), allowing direct observation of the efficiency of infection. Ad-*EGFP/Mad2* induced high expression of exogenous Mad2 (Fig. 3*A*) and did not affect the distribution of cells (MCF-7, T47D, Ovca432) among the various phases of the cell cycle statistically (χ test, $P > 0.05$ in all three cell lines; Fig. 3*B*).

First, we used *Mad2*-knockdown MCF-7 cells, which were shown to have a nonfunctional checkpoint (Fig. 1, *C* and *D*). The expression of Mad2 was restored in *Mad2*-knockdown cells by infection of Ad-*EGFP/Mad2* (Fig. 3*C*). Then, to determine

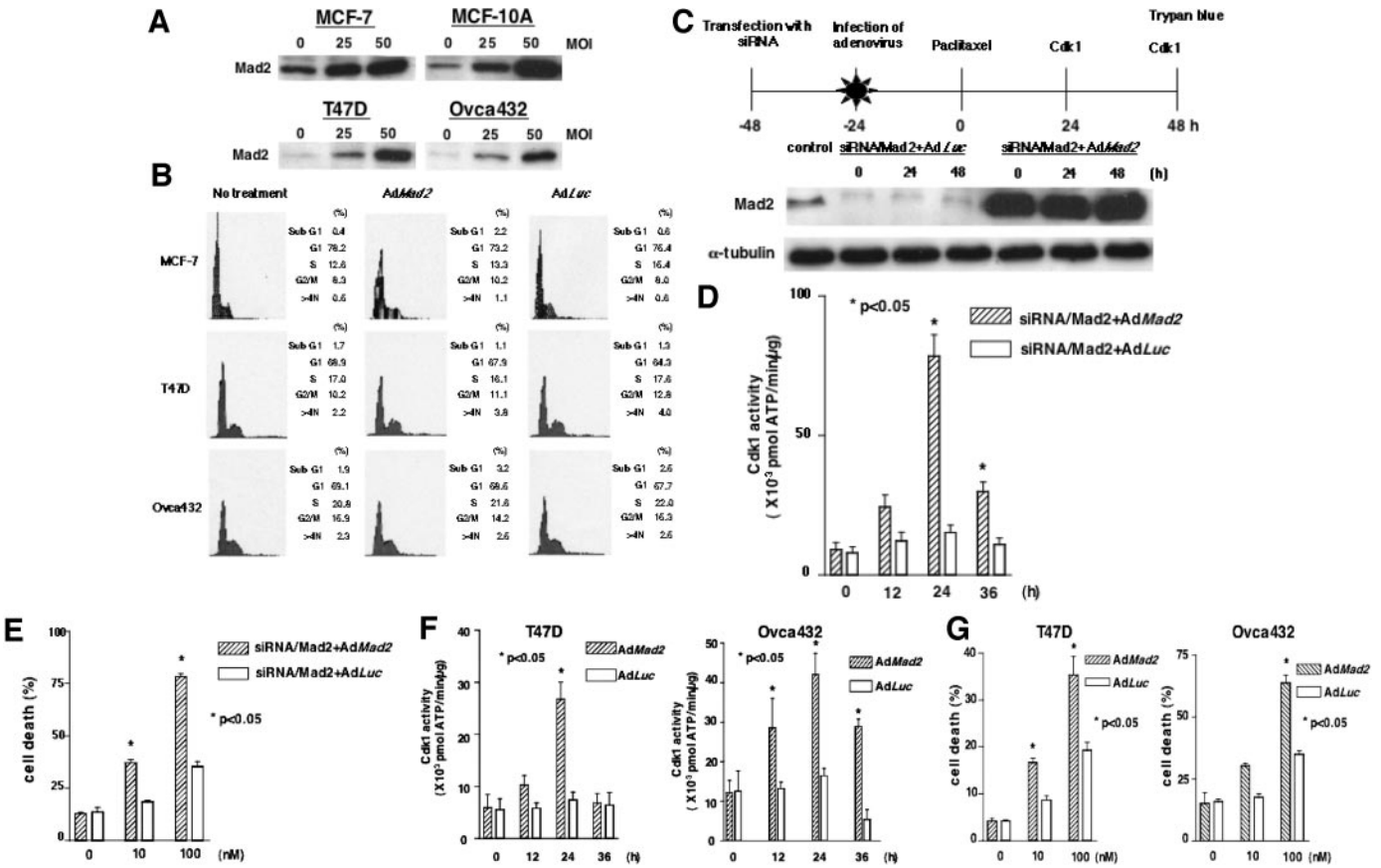

Fig. 3. Restoration of function of spindle assembly checkpoint and enhancement of paclitaxel sensitivity by overexpression of Mad2 in Mad2-dependent checkpoint-defective cells. *A*, exogenous Mad2 expression in MCF-7, MCF-10A, T47D, and Ovca432 cells by infection with Ad-*EGFP/Mad2* (Ad*Mad2*). Twenty-four h after infection at multiplicity of infection (MOI) values of 25 and 50, 20 μg of each lysate sample were applied and subjected to protein immunoblot analysis with anti-Mad2 antibody. *B*, no difference in cell cycle distribution by overexpression of Mad2. Cell cycle distribution of cells with overexpression of Mad2 as measured by DNA content by fluorescence-activated cell sorting. MCF-7, T47D, and Ovca432 cells were harvested 48 h after infection and subsequently stained with propidium iodide to detect DNA content. Numbers show the percentages of cells in each phase. Nonstatistical significance was determined in each cell line by χ^2 test (MCF-7, $P = 0.1011$; T47D, $P = 0.0789$; Ovca432, $P = 0.9581$). *Top of C*, schedule for combined small interfering RNA (siRNA)/*Mad2* transfection and adenovirus infection. Twenty-four h after transfection of siRNA/*Mad2*, adenoviral vectors (MOI of 50) were delivered over a 24-h period, and cells were exposed to paclitaxel (100 nM). *Bottom of C*, expression of Mad2 in Mad2-suppressed MCF-7 cells infected with Ad-*EGFP/Mad2* or Ad-*EGFP/Luc* (Ad*Luc*). Cells were harvested at 0, 24, and 48 h after paclitaxel treatment and subjected to protein immunoblot analysis with each antibody and α-tubulin antibody to control for gel loading. *D*, increased cyclin-dependent kinase-1 (Cdk1) activity after treatment with paclitaxel in Mad2-suppressed MCF-7 cells infected with Ad-*EGFP/Mad2* compared with Ad-*EGFP/Luc*-infected cells. Twenty-four h after infection with either Ad-*EGFP/Mad2* or Ad-*EGFP/Luc* at a MOI of 50, cells were treated with paclitaxel (100 nM) and harvested at the indicated times. Cdk1 activity in the lysate was determined as described in "Materials and Methods." *E*, recovered paclitaxel-induced cell death in Mad2-suppressed MCF-7 cells infected with Ad-*EGFP/Mad2*. Twenty-four h after infection, cells were harvested. Forty-eight h after treatment with paclitaxel, cell viability was assessed using trypan blue exclusion assay. *Bars*, SDs. *F*, increased Cdk1 activity after treatment with paclitaxel in Ad-*EGFP/Mad2*-infected T47D and Ovca432 cells. Twenty-four h after infection with either Ad-*EGFP/Mad2* or Ad-*EGFP/Luc* at a MOI of 50, cells were treated with paclitaxel (100 nM) and harvested at the indicated times. Cdk1 activity in the lysate was determined as described in "Materials and Methods." *G*, increased paclitaxel-induced cell death in T47D and Ovca432 cells infected with Ad-*EGFP/Mad2*. Cells were harvested 24 h after infection. Forty-eight h after treatment with paclitaxel, cell viability was assessed using trypan blue exclusion assay. *Bars*, SDs.

whether the function of the checkpoint can be restored by re-expression of Mad2, we assessed the activation of Cdk1 in Ad-*EGFP/Mad2*-infected *Mad2*-knockdown cells after paclitaxel treatment. The Cdk1 activity did not increase in the cells that had been infected with recombinant adenovirus, which expressed luciferase (Ad-*EGFP/Luc*) even after exposure to paclitaxel; these findings are consistent with the data presented in Fig. 1. In contrast, Cdk1 activity was restored in the Ad-*EGFP/Mad2*-infected cells, indicating that overexpression of Mad2 can restore the function of the spindle assembly checkpoint ($P < 0.05$; Fig. 3*D*). We then sought to determine whether this restoration enhanced the level of cell death induced by paclitaxel and found that paclitaxel-induced cell death (10, 100 nM) was, indeed, significantly higher in the Ad-*EGFP/Mad2*-infected cells than in the Ad-*EGFP/Luc*-infected cells ($P < 0.05$; Fig. 3*E*).

We also used T47D and Ovca432 cells, which are known to show the defective checkpoint because of low expression of Mad2 (12). Infection of these cell lines with Ad-*EGFP/Mad2* induced high expression levels of exogenous Mad2 and did not affect the cell cycle distribution (Fig. 3, *A* and *B*). The Cdk1 activity and paclitaxel sensitivity were higher in the Ad-*EGFP/Mad2*-infected cells than in the Ad-*Luc*-infected cells ($P < 0.05$; Fig. 3, *F* and *G*). These data demonstrate that exogenous Mad2 expression can restore the function of the checkpoint and enhance cell death in Mad2-dependent checkpoint-defective cells.

Effect of Mad2 Overexpression on Checkpoint Function and Paclitaxel Sensitivity in BubR1-Suppressed Cells. We then sought to determine whether overexpression of Mad2 could overcome spindle assembly checkpoint defects attributable to molecules other than Mad2. We used *BubR1*-knockdown MCF-7 cells, which were shown to be defective at the checkpoint (Fig. 1, *C* and *D*). Ad-*EGFP/Mad2* induced high expression of exogenous Mad2 and did not affect the expression of BubR1 in *BubR1*-knockdown cells (Fig. 4*A*). However, Cdk1 was not up-regulated in Ad-*EGFP/Mad2*-infected cells, and paclitaxel-induced cell death was not enhanced (Fig. 4, *B* and *C*). These data indicate that overexpression of Mad2 did not overcome the function of the checkpoint and paclitaxel sensitivity in cells with a Mad2-independent defective checkpoint.

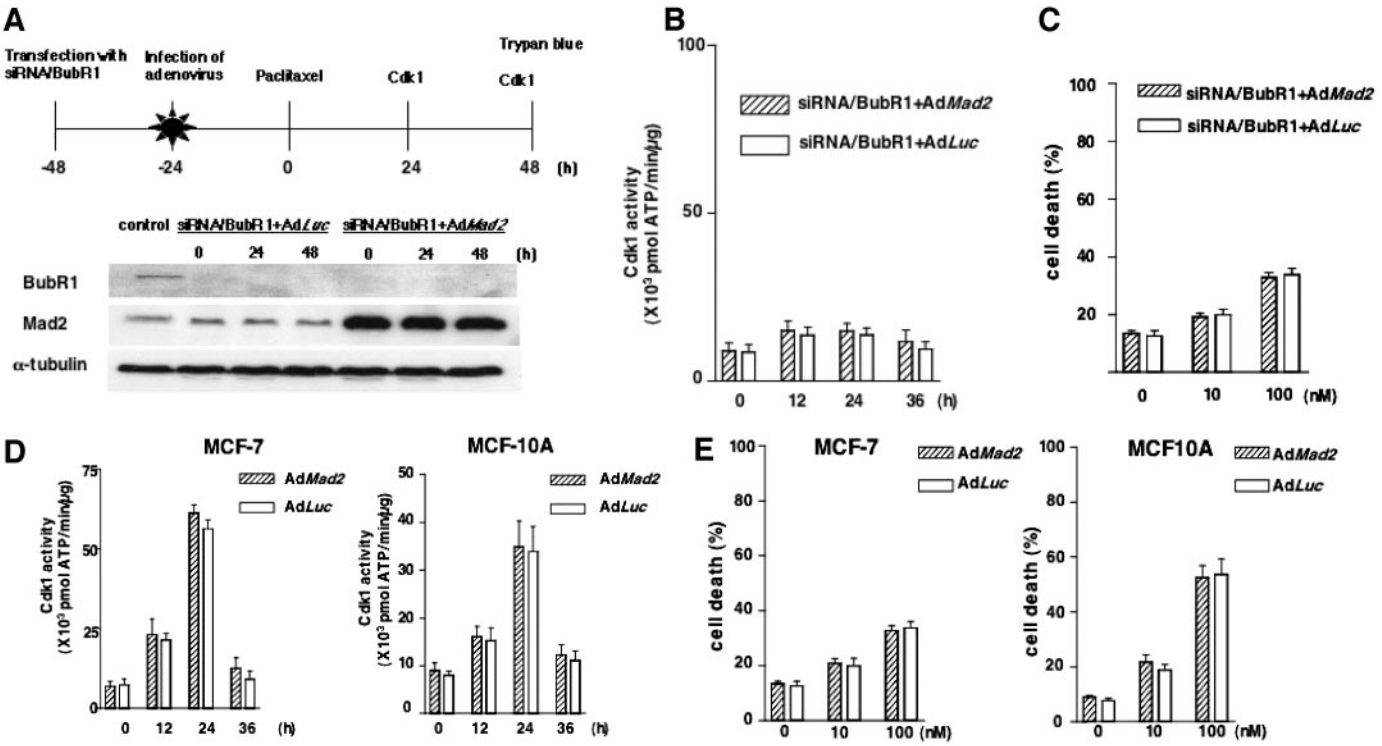

Fig. 4. Inability of Mad2 overexpression to enhance checkpoint function and paclitaxel sensitivity in cells with Mad2-independent defective or functional checkpoint. *Top of A*, schedule for combined small-interfering RNA (siRNA)/*BubR1* transfection and adenovirus infection. Twenty-four h after transfection of siRNA/*BubR1*, adenoviral vectors (multiplicity of infection of 50) were delivered over a 24-h period, and cells were exposed to paclitaxel (100 nM). *Bottom of A*, expression of Mad2 and BubR1 in BubR1-suppressed MCF-7 cells infected with Ad-*EGFP/Mad2* or Ad-*EGFP/Luc*. Cells were harvested at the indicated times after paclitaxel treatment and subjected to protein immunoblot analysis with each antibody and α-tubulin antibody to control for gel loading. *B*, cyclin-dependent kinase-1 (Cdk1) activity after treatment with paclitaxel in BubR1-suppressed MCF-7 cells infected with Ad-*EGFP/Mad2* or Ad-*EGFP/Luc*. Cells were harvested at the indicated times after paclitaxel treatment. Activity of Cdk1 in the lysate was determined as described in "Materials and Methods." *C*, paclitaxel-induced cell death in BubR1-suppressed MCF-7 cells infected with Ad-*EGFP/Mad2* or Ad-*EGFP/Luc*. Cells were harvested 48 h after treatment with paclitaxel. Cell viability was assessed by trypan blue exclusion. *Bars*, SDs. *D*, Cdk1 activity after treatment of paclitaxel in infected MCF-7 and MCF-10A cells. Twenty-four h after infection with Ad-*EGFP/Mad2* or Ad-*EGFP/Luc* at a multiplicity of infection of 50, cells were treated with paclitaxel (100 nM) and harvested at the indicated times. Cdk1 activity in the lysate was determined as described in "Materials and Methods." *E*, paclitaxel-induced cell death in MCF-7 and MCF-10A cells infected with Ad-*EGFP/Mad2* or Ad-*EGFP/Luc*. Cells were harvested 24 h after infection. Forty-eight h after treatment with paclitaxel, cell viability was assessed using trypan blue exclusion assay. *Bars*, SDs.

Effect of Overexpression of Mad2 on Checkpoint Function and Paclitaxel Sensitivity in Cells with a Functional Checkpoint. Finally, we sought to determine whether overexpression of Mad2 enhances the function of the spindle assembly checkpoint, a finding that could translate into enhanced paclitaxel-induced cell death in checkpoint-intact cells. In MCF-10A cells and MCF-7 cells, both of which are known to have a functional checkpoint, Ad-*EGFP/Mad2* effectively induced high expression levels of Mad2 (Fig. 3*A*). However, Cdk1 activity was not increased in Ad-*EGFP/Mad2*-infected cells of either cell line, and there was therefore no enhancement of paclitaxel-induced cell death (Fig. 4, *D* and *E*). Thus, overexpression of Mad2 failed to enhance the checkpoint functionality and paclitaxel sensitivity in cells with a basically functional spindle assembly checkpoint.

DISCUSSION

Our results highlight a specific role of the spindle assembly checkpoint for paclitaxel sensitivity. We showed that loss of the spindle assembly checkpoint suppressed paclitaxel-induced cell death, resulting in increased paclitaxel resistance. Therefore, paclitaxel resistance of certain tumors may be substantially attributable to defects in the spindle assembly checkpoint.

Previous studies have shown that on activation of the spindle assembly checkpoint, both Mad2 and BubR1 interact with Cdc20 directly and inhibit its ability to activate APC (16–19). APC-mediated destruction of cyclin B and other key regulators of mitosis is responsible for proper metaphase-to-anaphase transition and mitotic exit. The destruction of cyclin B results in the inactivation of Cdk1. The destruction of Pds1p (securin) releases Esp1 (separase) to degrade Mcd1p/Scc1p, a component of the cohesin complex that is important for sister chromatid cohesion. Proper control of Pds1/securin degradation ensures normal metaphase-to-anaphase transition and faithful chromosomal transmission during mitosis. When cells are exposed by spindle-inhibitors, the spindle assembly checkpoint activates and inhibits the degradation of cyclin B and securin; subsequently, cells arrest at pro-metaphase with persisting Cdk1 activity.

To determine whether suppression of Mad2 or BubR1 through transient knockdown in cell lines would affect the function of the spindle assembly checkpoint induced by paclitaxel, we performed gene silencing using siRNA duplexes. We found that suppression of Mad2 or BubR1 results in loss of accumulation of mitotic indices and inactivation of Cdk1 induced by paclitaxel. Moreover, concurrent suppression of Mad2 and BubR1 results in a reduction of the function of spindle assembly checkpoint similar to the reduction caused by suppression of either Mad2 or BubR1 alone. This finding suggests that depletion of either Mad2 or BubR1 is sufficient to abolish completely the function of the spindle assembly checkpoint. Recent reports have clearly demonstrated that every single, spindle assembly checkpoint gene thus far identified is essential for maintaining mitotic arrest (27–29). Mad2 and BubR1 act cooperatively in the mitotic checkpoint complex for the initiation and maintenance of the spindle assembly checkpoint (19), a finding that appears consistent with our results. Moreover, transfection of MDA-MB-231 and SKBr-3 cells, which

have a functional spindle assembly checkpoint, with siRNA/*Mad2*, siRNA/*BubR1*, or both resulted in loss of the checkpoint and resistance to paclitaxel—effects similar to those in MCF-7 cells (data not shown). These cell lines are known to have mutated p53 and HER-2/*neu* overexpression respectively. Despite these known genetic differences, abolishment of the spindle assembly checkpoint resulted in similar findings of resistance to paclitaxel.

Although no *Mad2* mutations have been detected in cancer cell lines with checkpoint defects, few reports on the expression level of Mad2 protein in human specimens have been published (30). Some types of cancer cells may have a nonfunctional checkpoint because of low expression of Mad2. In the present study, we found that Mad2 overexpression enhances paclitaxel-induced cell death via enhancement of checkpoint activation. Overexpression of Mad2 augmented Cdk1 activity and paclitaxel-induced cell death in cells that have a spindle assembly checkpoint that is nonfunctional because of low Mad2 expression (*i.e.*, T47D and Ovca432 cells).

However, overexpression of Mad2 does not appear to improve either Cdk1 activity or paclitaxel sensitivity in cells with a checkpoint defect attributable to low expression of a gene other than *Mad2* (*e.g.*, *BubR1*). In other experiments, we have found that the function and cytotoxicity were not enhanced by overexpression of Mad2 in the SW480 colorectal cancer cell line, which is known to have a defective spindle assembly checkpoint (data not shown). These data may suggest that every single known gene associated with the spindle assembly checkpoint is indispensable for proper function of the checkpoint. Our data provide a preclinical basis for using *Mad2* as a therapeutic gene in combination with paclitaxel in those patients with dysfunctional *Mad2*. More important, however, is that our data show that any molecules that could interfere with the spindle assembly checkpoint could generate paclitaxel resistance in any patient.

Finally, we found that overexpression of Mad2 fails to enhance Cdk1 activity and paclitaxel sensitivity in cells having a functional checkpoint (*i.e.*, MCF-7 and MCF-10A cells). Previous reports have shown that deletion of one *Mad2* allele results in a defective spindle assembly checkpoint (31) and that Mad2 must be recruited to the kinetochores via its interaction with Mad1 and inhibition of APC/Cdc20 (32, 33). These results suggest that a certain quantity and a specific localization of Mad2 are required for Mad2 to act as a component in the spindle assembly checkpoint machinery, and that large quantities of Mad2 may not be necessary for enhancement of the function of the checkpoint.

Because losses or gains of chromosomes are hallmarks in human cancers, we suspect that the spindle assembly checkpoint is frequently lost in the clinical setting. Despite many reports of detection of spindle assembly checkpoint defects in human lung, colorectal, ovarian, and nasopharyngeal cancer cell lines *in vitro* (24, 25, 34–36), mutations in known spindle assembly checkpoint genes occur very rarely in human cancers (35–38). This paradox may be explained by various post-transcriptional or post-translational modifications to checkpoint complexes. Moreover, because the spindle assembly checkpoint machinery consists of various molecules, assessing the function of the checkpoint in human cancer samples by analyzing mutations of genes or protein expressions would be impractical.

In summary, our data support the notion that the induction of dysfunctional spindle assembly checkpoint by knocking down *Mad2* and/or *BubR1* results in resistance to paclitaxel. This is some of the first direct evidence that functional spindle assembly checkpoint is essential for paclitaxel-sensitivity. The next step in this research will be to determine how we can measure the function of the spindle assembly checkpoint in human cancer cells. We also have shown that insufficient elevation of Cdk1 activity correlates with paclitaxel resistance. We plan to monitor the activity of Cdk1 in tumor samples from patients treated with paclitaxel to show that increased Cdk1 after the first dose of paclitaxel may be a useful marker to predict which tumors will respond to the drug.

ACKNOWLEDGMENTS

We thank Dr. Mien-Chie Hung for critical review of the manuscript; K. Ó Súilleabháin for excellent help in editing this manuscript; Drs. H. Itamochi, T. Takahashi, and C. Bartholomeusz for helpful and constructive discussions; and S. Das for assistance.

REFERENCES

1. Eifel P, Axelson JA, Costa J, et al. National Institutes of Health Consensus Development Conference Statement: adjuvant therapy for breast cancer, November 1–3, 2000. J Natl Cancer Inst (Bethesda) 2001;93:979–89.
2. Holmes FA, Walters RS, Theriault RL, et al. Phase II trial of taxol, an active drug in the treatment of metastatic breast cancer. J Natl Cancer Inst (Bethesda) 1991;83:1797–1805.
3. Nabholtz JM, Gelmon K, Bontenbal M, et al. Multicenter, randomized comparative study of two doses of paclitaxel in patients with metastatic breast cancer. J Clin Oncol 1996;14:1858–67.
4. Bishop JF, Dewar J, Toner GC, et al. Initial paclitaxel improves outcome compared with CMFP combination chemotherapy as front-line therapy in untreated metastatic breast cancer. J Clin Oncol 1999;17:2355–64.
5. McGuire WP, Hoskins WJ, Brady MF, et al. Cyclophosphamide and cisplatin compared with paclitaxel and cisplatin in patients with stage III and stage IV ovarian cancer. N Engl J Med 1996;334:1–6.
6. Piccart MJ, Bertelsen K, James K, et al. Randomized intergroup trial of cisplatin-paclitaxel versus cisplatin-cyclophosphamide in women with advanced epithelial ovarian cancer: three-year results. J Natl Cancer Inst (Bethesda) 2000;92:699–708.
7. Tang C, Willingham MC, Reed JC, et al. High levels of p26BCL-2 oncoprotein retard taxol-induced apoptosis in human pre-B leukemia cells. Leukemia 1994;8:1960–9.
8. Huang Y, Ibrado AM, Reed JC, et al. Co-expression of several molecular mechanisms of multidrug resistance and their significance for paclitaxel cytotoxicity in human AML HL-60 cells. Leukemia 1997;11:253–7.
9. Giannakakou P, Sackett DL, Kang YK, et al. Paclitaxel-resistant human ovarian cancer cells have mutant β-tubulins that exhibit impaired paclitaxel-driven polymerization. J Biol Chem 1997;272:17118–25.
10. Yu D, Jing T, Liu B, et al. Overexpression of ErbB2 blocks Taxol-induced apoptosis by upregulation of p21Cip1, which inhibits p34Cdc2 kinase. Mol Cell 1998;2:581–91.
11. Yu H. Regulation of APC-Cdc20 by the spindle checkpoint. Curr Opin Cell Biol 2002;14:706–14.
12. Li Y, Benezra R. Identification of a human mitotic checkpoint gene: hsMAD2. Science (Wash D C) 1996;274:246–8.
13. Jin DY, Spencer F, Jeang KT. Human T cell leukemia virus type 1 oncoprotein Tax targets the human mitotic checkpoint protein MAD1. Cell 1998;93:81–91.
14. Taylor SS, Ha E, McKeon F. The human homologue of Bub3 is required for kinetochore localization of Bub1 and a Mad3/Bub1-related protein kinase. J Cell Biol 1998;142:1–11.
15. Chan GK, Jablonski SA, Sudakin V, Hittle JC, Yen TJ. Human BUBR1 is a mitotic checkpoint kinase that monitors CENP-E functions at kinetochores and binds the cyclosome/APC. J Cell Biol 1999;146:941–54.
16. Fang G, Yu H, Kirschner MW. The checkpoint protein MAD2 and the mitotic regulator CDC20 form a ternary complex with the anaphase-promoting complex to control anaphase initiation. Genes Dev 1998;12:1871–83.
17. Sudakin V, Chan GK, Yen TJ. Checkpoint inhibition of the APC/C in HeLa cells is mediated by a complex of BUBR1, BUB3, CDC20, and MAD2. J Cell Biol 2001;154:925–36.
18. Tang Z, Bharadwaj R, Li B, Yu H. Mad2-Independent inhibition of APCCdc20 by the mitotic checkpoint protein BubR1. Dev Cell 2001;1:227–37.
19. Fang G. Checkpoint protein BubR1 acts synergistically with Mad2 to inhibit anaphase-promoting complex. Mol Biol Cell 2002;13:755–66.
20. Nigg EA. Mitotic kinases as regulators of cell division and its checkpoints. Nat Rev Mol Cell Biol 2001;2:21–32.
21. Meikrantz W, Schlegel R. Suppression of apoptosis by dominant negative mutants of cyclin-dependent protein kinases. J Biol Chem 1996;271:10205–9.
22. Shen SC, Huang TS, Jee SH, Kuo ML. Taxol-induced p34cdc2 kinase activation and apoptosis inhibited by 12-O-tetradecanoylphorbol-13-acetate in human breast MCF-7 carcinoma cells. Cell Growth Differ 1998;9:23–9.
23. He TC, Zhou S, da Costa LT, Yu J, Kinzler KW, Vogelstein B. A simplified system for generating recombinant adenoviruses. Proc Natl Acad Sci USA 1998;95:2509–14.
24. Takahashi T, Haruki N, Nomoto S, Masuda A, Saji S, Osada H. Identification of frequent impairment of the mitotic checkpoint and molecular analysis of the mitotic checkpoint genes, hsMAD2 and p55CDC, in human lung cancers. Oncogene 1999;18:4295–300.
25. Wang X, Jin DY, Wong YC, et al. Correlation of defective mitotic checkpoint with aberrantly reduced expression of MAD2 protein in nasopharyngeal carcinoma cells. Carcinogenesis 2000;21:2293–7.
26. Wang X, Jin DY, Ng RW, et al. Significance of MAD2 expression to mitotic checkpoint control in ovarian cancer cells. Cancer Res 2002;62:1662–8.

27. Dobles M, Liberal V, Scott ML, Benezra R, Sorger PK. Chromosome missegregation and apoptosis in mice lacking the mitotic checkpoint protein Mad2. Cell 2000;101: 635–45.
28. Kalitsis P, Earle E, Fowler KJ, Choo KH. Bub3 gene disruption in mice reveals essential mitotic spindle checkpoint function during early embryogenesis. Genes Dev 2000;14:2277–82.
29. Luo X, Tang Z, Rizo J, Yu H. The Mad2 spindle checkpoint protein undergoes similar major conformational changes upon binding to either Mad1 or Cdc20. Mol Cell 2002;9:59–71.
30. Tanaka K, Nishioka J, Kato K, et al. Mitotic checkpoint protein hsMAD2 as a marker predicting liver metastasis of human gastric cancers. Jpn J Cancer Res 2001;92: 952–8.
31. Michel LS, Liberal V, Chatterjee A, et al. MAD2 haplo-insufficiency causes premature anaphase and chromosome instability in mammalian cells. Nature (Lond) 2001; 409:355–9.
32. Chen RH, Shevchenko A, Mann M, Murray AW. Spindle checkpoint protein Xmad1 recruits Xmad2 to unattached kinetochores. J Cell Biol 1998;143:283–95.
33. Waters JC, Chen RH, Murray AW, Salmon ED. Localization of Mad2 to kinetochores depends on microtubule attachment, not tension. J Cell Biol 1998;141:1181–91.
34. Cahill DP, Lengauer C, Yu J, et al. Mutations of mitotic checkpoint genes in human cancers. Nature (Lond) 1998;392:300–3.
35. Nakagawa H, Yokozaki H, Oue N, et al. No mutations of the Bub1 gene in human gastric and oral cancer cell lines. Oncol Rep 2002;9:1229–32.
36. Saeki A, Tamura S, Ito N, et al. Frequent impairment of the spindle assembly checkpoint in hepatocellular carcinoma. Cancer (Phila) 2002;94:2047–54.
37. Sato M, Sekido Y, Horio Y, et al. Infrequent mutation of the hBUB1 and hBUBR1 genes in human lung cancer. Jpn J Cancer Res 2000;91:504–9.
38. Haruki N, Saito H, Harano T, et al. Molecular analysis of the mitotic checkpoint genes BUB1, BUBR1 and BUB3 in human lung cancers. Cancer Lett 2001;162:201–5.

Dependence of Paclitaxel Sensitivity on a Functional Spindle Assembly Checkpoint

Tamotsu Sudo, Masayuki Nitta, Hideyuki Saya, et al.

Cancer Res 2004;64:2502-2508.